Colloid Polym Sci 279:292–296 (2001)

SHORT COMMUNICATION

X. Zhu
Y. Li
D. Yan
P. Zhu
Q. Lu

Influence of the order of polymer melt on the crystallization behavior: I. Double melting endotherms of isotactic polypropylene

Received: June 16, 2000
Accepted: October 16, 2000

X. Zhu · Y. Li · D. Yan (✉)
College of Chemistry
and Chemical Technology
Shanghai Jiao Tong University
800 Dongchuan Road
Shanghai 200240
People's Republic of China
e-mail: dyyan@mail.sjtu.edu.cn
Tel.: +86-21-5474-2665
Fax: +86-21-5474-1297

P. Zhu · Q. Lu
Instrumental Analysis Center
Shanghai Jiao Tong University
1954 Huashan Road, Shanghai 200030
People's Republic of China

Abstract The influence of the order of polymer melt on the subsequent crystallization and melting has been carefully studied. The experimental data show that the order of isotactic polypropylene (iPP) melt decreases with increases in the fusion temperature. For an iPP sample isothermally crystallized at 130 °C for half an hour, the degree of order of melt is higher when the fusion temperature is lower than about 170.5 °C, hence the lamellae formed in a rapid cooling process are perfect. If the fusion temperature is not higher than 167 °C, some thicker lamellae can exist in the melt. The melting of these unmelted lamellae and those lamellae recrystallized in the cooling process result in double endotherms. On the other hand, when the fusion temperature is higher than 170.5 °C, the order of the iPP melt decreases greatly; thus, the lamellae formed in the following cooling process are imperfect. At a lower heating rate, the recrystallization or reorganization of these imperfect lamellae also leads to double melting endotherms.

Key words The order of melt · Crystallization · Melting · Double endotherms

Introduction

The effect of fusion temperature on the crystallization and melting behaviors of iPP has been extensively studied for a long time. Many researchers [1–5] have found that the rate constants for the crystallization decrease with increasing fusion temperature. Provided the fusion temperature amounts to 200 °C and above the Avrami exponent, for suitable crystallization temperatures, increases from 3 to 4, indicating the change from athermal to thermal nucleation [4–6]. Fillon et al. [7] have investigated the crystallization behavior of iPP after partial and complete melting. They observed that, after melting in a lower temperature and recrystallization, the polymers display a prominent morphological memory effect. Recently, Alfonso and Ziabicki [8, 9] have studied the memory effect of iPP in isothermal crystallization, and propose that the gradual destruction of large clusters (crystal aggregates) in the iPP melt is the main factor responsible for the effect of melting history on isothermal crystallization.

Almost all the works mentioned above attribute the changes of crystallization and melting behaviors to the residual crystallites in the melt, and no attention is paid to the variations of the molecular structure of the iPP melt itself. The purpose of this paper is to analyze the influence of the order of the iPP melt on the crystallization and melting behaviors, and to elucidate the origins of the double melting endotherms corresponding to the different temperature regions.

Materials and methods

The isotactic polypropylene (iPP) used in this study had an isotacticity of 94.5%. The melt flow index was 3.0 g/10 min. A film of polymer was melted at 210 °C for 10 min, and then crystallized at 130 °C for half an hour. Finally, the sample was quenched to 0 °C.

Thermal measurements were carried out on a Perkin-Elmer Pyris-1 Series differential scanning calorimeter under a flowing nitrogen atmosphere. The DSC was carefully calibrated with In and Zn standards; the constancy of the calibration was checked every second or third run. For all experiments the sample weights were approximately 5 mg. The obtained results show that the melting point of the iPP sample, that was isothermally crystallized at 130 °C for half an hour, was 161.3 °C at the heating rate of 5 °C/min.

The IR spectra were collected at a resolution of 4.0 cm^{-1} using a Bruker Equinox-55 FTIR spectrometer equipped with a variable temperature cell. The sample was heated from room temperature (20 °C) to 210 °C at a heating rate of 5 °C/min. At the same time, the FTIR spectra were recorded at the rate of 1 spectrum per 10 seconds. Thus, the relationship of intensity with temperature can be obtained and the details have been well described in our previous papers [10, 11]. The scanned wave number range was 4000–400 cm^{-1}.

Raman spectra were recorded on a Bruker FRA 106/S FT-Raman spectrometer at room temperature (20 °C). The 1064 nm line from an yttrium-aluminum garnet laser doped with neodymium was used for excitation. The scanned wave number range was 3500–50 cm^{-1}.

Wide angle X-ray diffraction (WAXD) experiments were performed with a Rigaku III Dmax 2500 diffractometer in the deflection mode at 35 kV and 25 mA. Nickel-filtered Cu-Kα radiation was used in all cases.

Results and discussion

It has been well established that the regularity bands of a polymer originate from the intramolecular coupling of oscillations of the various atomic groups [12]. The major proportion of the iPP molecules are in a 3_1 helix conformation and the 1220, 841 and 998 cm^{-1} bands all belong to the regularity bands. These bands are related to the different helical lengths of isotactic sequences [10, 13–18]. Concerning the 973 cm^{-1} band, it has been well established that this band is not only attributed specifically to the PP head-to-tail sequence of the repeating units, but also is associated with the presence of short isotactic helices [19]. The minimum "n" values for appearance of the 973, 998, 841 and 1220 cm^{-1} bands are 2–4, 5–10, 12–14, and 14 or more monomer units in the helical sequences, respectively [13–19]. Therefore, the conformational order of different iPP samples can be determined by the absorbance ratio of the various regularity bands. Figure 1 shows a the plot of the normalized intensity of the various regularity bands with temperature for an iPP sample at the heating rate of 5 °C/min. It can be deduced that the IR intensity decreases approximately linearly with increases in temperature below 170.5 °C. When the temperature is higher than about 170.5 °C, a large loss in intensity occurs, indicating abrupt jumps in the concentration of helical regularity structure. During the heating process, the 1220 cm^{-1} band disappears first, and then the 841 cm^{-1} band. The 998 cm^{-1} band is considerably weakened while that at 973 cm^{-1} is almost unchanged. Apparently, the band with longer helical sequences disappears more quickly, which demonstrates that the order of the polymer melt decreases successively with enhancing of the temperature. This result can be further confirmed by Fig. 2, in which the absorbance ratios of $A_{1220\mathrm{cm}^{-1}}/A_{841\mathrm{cm}^{-1}}$, $A_{841\mathrm{cm}^{-1}}/A_{998\mathrm{cm}^{-1}}$, and $A_{998\mathrm{cm}^{-1}}/A_{973\mathrm{cm}^{-1}}$ also decrease successively with increasing the temperature. For an iPP sample isothermally crystallized at 130 °C for half an hour, the DSC measurement reveals that the melting point is 161.3 °C at the heating rate of 5 °C/min. On heating this sample to a different fusion temperature (T_f) higher than the melting point, an iPP melt with a different conformational order will be formed. On cooling the melt to room temperature at 40 °C/min, recrystallization occurs and the crystallites obtained should be of a different degree of perfection. The subsequent re-melting curves are shown in Fig. 3. It is very interesting to note that double melting endotherms appear at both higher and lower fusion

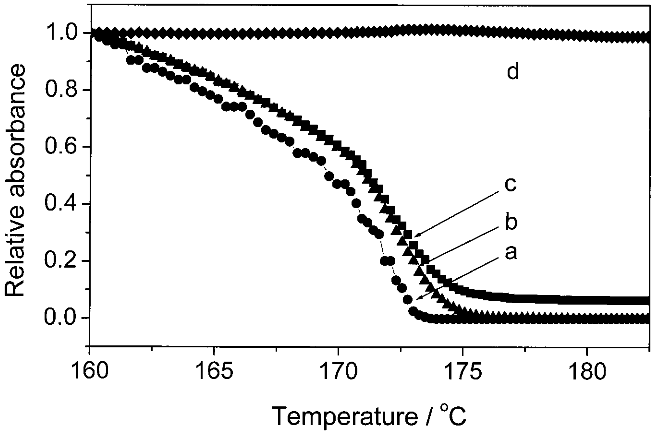

Fig. 1 Temperature dependence of the infrared bands near: (a) 1220 cm^{-1}; (b) 841 cm^{-1}; (c) 998 cm^{-1}; (d) 973 cm^{-1} in iPP at the heating rate of 5 °C/min

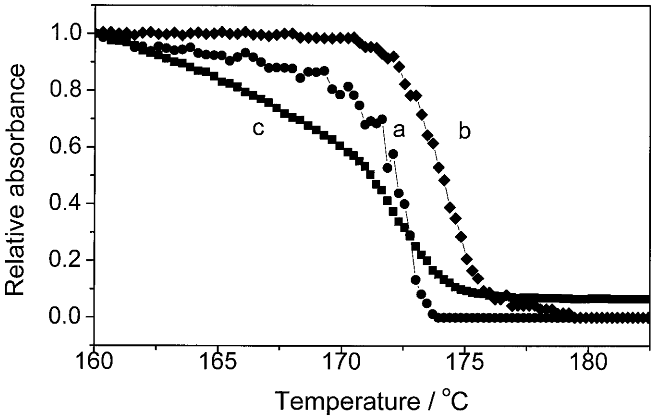

Fig. 2 The plot of intensity ratios of different infrared bands vs. temperature at the heating rate of 5 °C/min: (a) $A_{1220\mathrm{cm}^{-1}}/A_{841\mathrm{cm}^{-1}}$; (b) $A_{841\mathrm{cm}^{-1}}/A_{998\mathrm{cm}^{-1}}$; (c) $A_{998\mathrm{cm}^{-1}}/A_{973\mathrm{cm}^{-1}}$

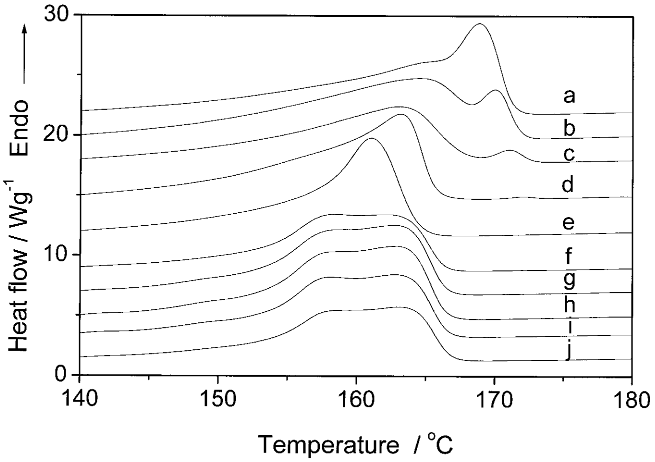

Fig. 3 The melting thermographs of an iPP sample that was heated to different fusion temperature: (a) 161.5 °C; (b) 163 °C; (c) 165 °C; (d) 167 °C; (e)169 °C; (f) 171 °C; (g) 173 °C; (h) 175 °C; (i) 177 °C; (j) 179 °C, cooled to 20 °C at 40 °C/min and then re-heated to 180 °C at 10 °C/min

temperatures, while only a single melting endotherm exists for the moderate fusion temperature. On the basis of the similarity in melting behaviors, the fusion temperature can be classified into three domains: domain I ($T_f \le 167$ °C), domain II (167 °C $< T_f <$ 171 °C), and domain III ($T_f \ge 171$ °C). The three cases are separately discussed below.

Domain I ($T_f \le 167$ °C)

Figure 3 shows that the double melting endotherms appear in this domain. With increasing fusion temperature, the area of the endotherm on the higher temperature side decreases and the peak temperature becomes higher, while the peak temperature on the lower temperature side decreases. Since the melting point of an iPP sample isothermally crystallized at 130 °C for half an hour is only 161.3 °C at the heating rate of 5 °C/min, it is possible that some thicker lamellae still exist in melt when the fusion temperature is only slightly higher than the melting point. Figure 4, trace a is the WAXD pattern measured at 163 °C. The strong equatorial diffraction peaks at $2\theta = 13.83°$, 16.90°, and 18.34° corroborate the existence of unmelted lamellae [20]. Therefore, the endotherm at higher temperature in domain I corresponds to the melting of these unmelted lamellae whereas the larger peak at lower temperature is produced by the melting of recrystallized lamellae formed in the cooling process. With increasing fusion temperature, the amount of unmelted lamellae becomes less and less and the residual lamellae are thicker and thicker, so the corresponding area of the melting endotherm on the higher temperature side decreases gradually and the melting peak shifts to the higher temperature. Furthermore, both Fig. 1 and Fig. 2 show that when the fusion temperature is lower than 170.5 °C, the conformational order of the polymer melt decreases slowly, thus the melting temperature of the lower endotherm decreases with the increase of the fusion temperature. Figure 5 shows the plot of normalized intensity of different regularity bands vs. time after the iPP sample had been heated to 163 °C at 5 °C/min. It reveals that the intensities of the various regularity bands change slightly with the time, suggesting that the conformational order of the iPP melt is almost unchanged during the retention periods. Therefore, the structure of the iPP melt is almost in equilibrium. Consequently, the peak temperature on the lower temperature side in Fig. 6 changes only slightly with the retention time. However, due to the lamellae thickening, the peak temperature in the higher temperature region increases gradually with increasing annealing time at 163 °C.

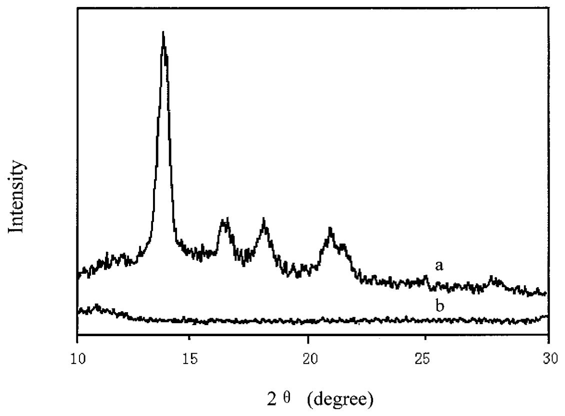

Fig. 4 Wide angle X-ray diffraction patterns of iPP measured at: (a) 163 °C; (b) 169 °C

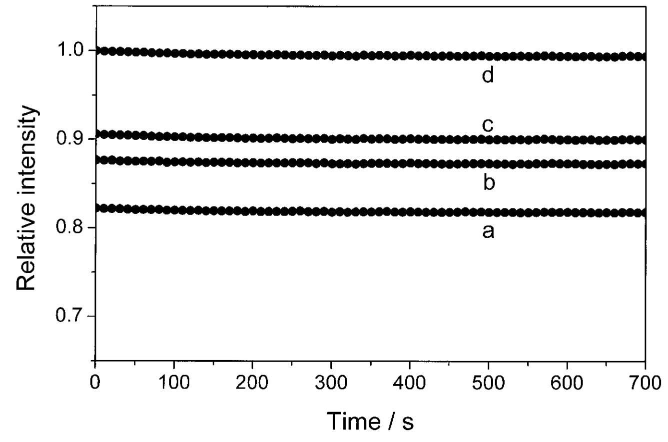

Fig. 5 The plot of the relative intensities of different infrared bands vs. time after the iPP sample had been heated to 163 °C at 5 °C/min: (a) 1220 cm^{-1}; (b) 841 cm^{-1}; (c) 998 cm^{-1}; (d) 973 cm^{-1}. The normalized intensity at 160 °C was set to unity

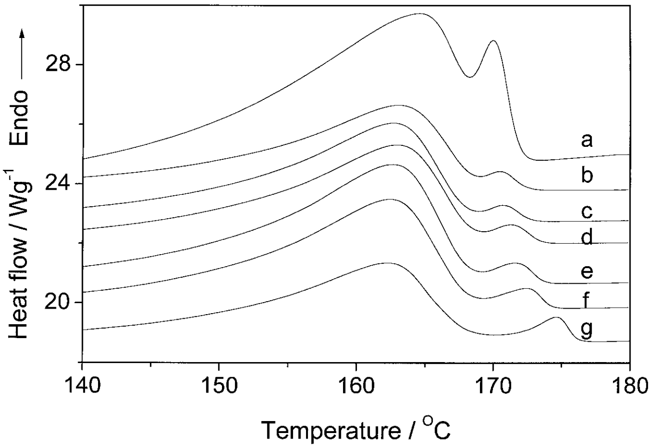

Fig. 6 The melting thermographs of an iPP sample that was heated to 163 °C at 5 °C/min, and held for different periods of time: (a) 0 min; (b) 0.5 min; (c) 1 min; (d) 1.5 min; (e) 2 min; (f) 3 min; (g) 10 min, cooled to 20 °C at 40 °C/min and then re-heated to 180 °C at 10 °C/min

Domain II (167 °C < T_f < 171 °C)

In this domain, only one melting endotherm appears. Compared with those melting curves in domain I, it can be found that the melting peak on the high temperature side has disappeared, which illustrates that all of the lamellae have melted when T_f > 167 °C. Figure 4, trace b is the WAXD pattern measured at 169 °C. There is no any sharp diffraction peak in this diffractogram, corroborating the absence of unmelted lamellae in the melt. Obviously, the single melting endotherm comes from the melting of recrystallized lamellae formed in the cooling process. Figures 1 and 2 show that, when the fusion temperature is lower than 170.5 °C, the conformational order of the iPP melt decreases with increasing the temperature, thus the corresponding peak temperature of melting endotherm decreases. If the iPP sample was heated to 169 °C and then held for 10 min, the IR measurements demonstrate that the intensities of thevarious regularity bands change slightly with the retention time, implying that the retention periods have little effect on the conformational order of the iPP melt. Figure 7 shows the melting curves of an iPP sample that was heated to 169 °C at 5 °C/min, held for different periods of time and then cooled to room temperature at 40 °C/min. Since the conformational order of melt is almost unchanged during the retention periods, the corresponding melting temperatures are similar to each other.

Domain III (T_f ≥ 171 °C)

Double melting endotherms also appear when the fusion temperature is equal to or higher than 171 °C. Figures 1 and 2 have pointed out that, when the temperature is higher than about 170.5 °C, the helical regularity structure of iPP molecules is reduced dramatically. This fact indicates that at a higher fusion temperature the polymer chains in the iPP melt have a lower conformational order. Such a molecular structure would favor the formation of crystallites of a lower degree of perfection and may introduce some defects into the crystallized zone. Consequently, it can be inferred that the double melting endotherms in domain III may result from recrystallization or reorganization. Figure 8 shows the melting thermograph of an iPP sample that was cooled

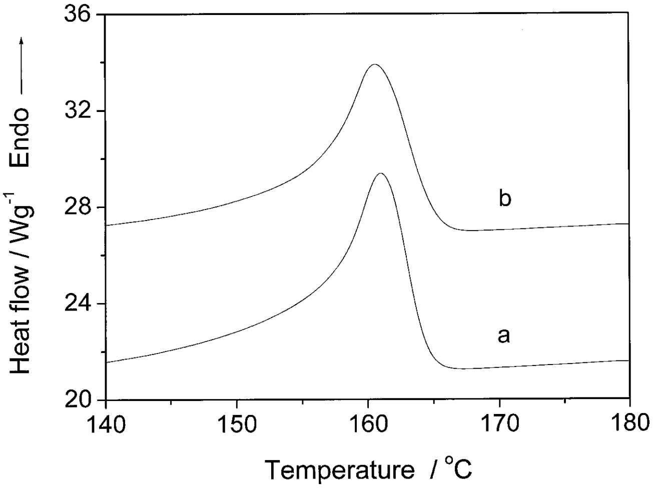

Fig. 7 The melting thermographs of an iPP sample that was heated to 169 °C at 5 °C/min, and held for different periods of time: (a) 0 min; (b) 10 min, cooled to 20 °C at 40 °C/min and then re-heated to 180 °C at 10 °C/min

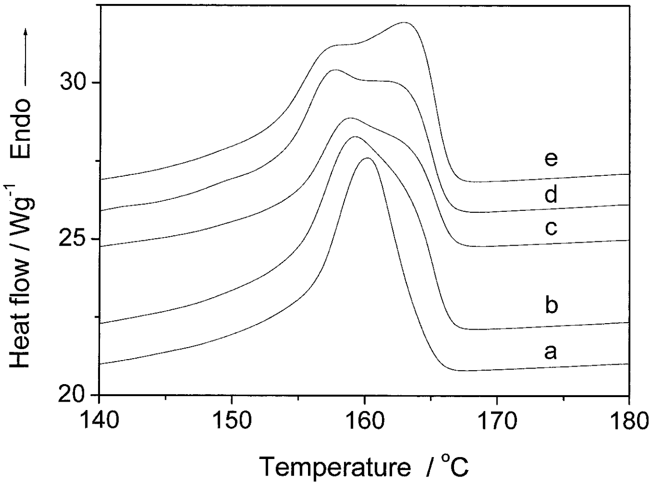

Fig. 8 The melting thermographs of an iPP sample that was heated to 179 °C at 5 °C/min, cooled to 20 °C at different cooling rates: (a) 5 °C/min; (b) 10 °C/min; (c) 15 °C/min; (d) 20 °C/min; (e) 40 °C/min, and then re-heated to 180 °C at 10 °C/min

Table 1 Relative ratios of different helix lengths in iPP samples that were crystallized at 130 °C for half an hour, heated to different fusion temperatures and then cooled to 20 °C at 40 °C/min

Fusion temperature (°C)	FTIR measurements		FT-Raman measurements	
	998:841:1220 cm^{-1}	841:1220 cm^{-1}	998:841:1220 cm^{-1}	841:1220 cm^{-1}
163	1:0.993:0.086	1:0.086	1:3.346:1.457	1:0.435
169	1:0.987:0.077	1:0.078	1:2.988:1.265	1:0.423
179	1:0.851:0.065	1:0.076	1:2.900:1.222	1:0.421
210	1:0.846:0.031	1:0.037	1:2.597:0.910	1:0.350

from 179 °C to room temperature (20 °C) at different cooling rates. On decreasing the cooling rate, the area of the endotherm on the lower temperature side increases at the expense of the area of the endotherm on the higher temperature side. Finally, only one endotherm appears at a very slow cooling rate. However, the sum of the two areas is found to be more or less independent of the cooling rate. Moreover, the lower melting peak shifts towards the high temperature region with a decreasing cooling rate whereas the higher melting peak is almost unchanged. These experimental data validate that the double melting endotherms in domain III result from recrystallization or reorganization [20]. The peak on the lower temperature represents the melting of the imperfect lamellae formed during the cooling process, while the peak on the higher temperature is due to the melting of more stable lamellae derived from recrystallization or reorganization of imperfect lamellae.

From the above discussion, it can be concluded that the fusion temperature has an important effect on the subsequent crystallization and melting behaviors. With increasing fusion temperature, the order of the polymer melt decreases, which restricts the formation of the long helical sequences in a fast cooling process. Additional evidence comes from the FTIR and FT-Raman spectroscopic analyses. Table 1 presents the relative ratios of the different helix lengths in an iPP sample that was heated to different fusion temperatures and then cooled to room temperature at 40 °C/min. Both the infrared and the Raman spectroscopic studies prove that the proportion of long helical sequences decreases with increasing fusion temperature.

Acknowledgements This work was subsidized by the Special Funds for Major State Basic Research Projects of China (G1999064800) and by Bruker Co.

References

1. Marker L, Hay PM, Tilley GP, Early RM, Sweeting OJ (1959) J Polym Sci 38:33
2. Yoshizaki O, Ishibashi T, Nagai E (1962) J Chem Soc Japan Ind Chem Sect 65:1614
3. Chiu J (1964) Anal Chem 36:2058
4. Majer J (1960) Kunstoffe 50:565
5. Parrini P, Corrieri G (1963) Makrom Chem 62:83
6. Parrini P, Corrieri G (1967) Chim Ind 49:1172
7. Fillon B, Wittmann JC, Lotz B, Thierry A (1993) J Polym Sci B Polym Phys 31:1383
8. Alfonso GC, Ziabicki A (1995) Colloid Polym Sci 273:317
9. Ziabicki A, Alfonso GC (1994) Colloid Polym Sci 272:1027
10. Zhu XY, Yan DY, Yao HX, Zhu PF (2000) Macromol Rapid Commun 21:354
11. Zhu XY, Yan DY. Macromol Chem Phys accepted
12. Zerbi G, Ciampelli F, Zamboni V (1963) J Polym Sci Part C 7:141
13. Kobayashi M, Akita K, Tadokoro H (1968) Makromol Chem 118:324
14. Miyamoto T, Inagaki H (1969) J Polym Sci Part A-2 7:963
15. Kissin YV, Tsvetkova VI, Chirkov NM (1972) Eur Polym J 8:529
16. Kissin YV, Rishina LA (1976) Eur Polym J 12:757
17. Hanna LA, Hendra PJ, Maddams W, Willis HA, Zichy V, Cudby MEA (1988) Polymer 29:1843
18. Passingham C, Hendra PJ, Cudby MEA, Weller M (1990) Eur Polym J 26:631
19. Burfield DR, Loi PST (1988) J Appl Polym Sci 36:279
20. Zhu XY, Yan DY, Tan SS, Wang T, Yan DH, Zhou E (2000) J Appl Polym Sci 77:163